

Hydrogen plasma-mediated modification of the electrical transport properties of ZnO nanowire field effect transistors

This content has been downloaded from IOPscience. Please scroll down to see the full text.

2015 Nanotechnology 26 125202

(<http://iopscience.iop.org/0957-4484/26/12/125202>)

View [the table of contents for this issue](#), or go to the [journal homepage](#) for more

Download details:

IP Address: 147.46.44.132

This content was downloaded on 07/07/2015 at 04:39

Please note that [terms and conditions apply](#).

Hydrogen plasma-mediated modification of the electrical transport properties of ZnO nanowire field effect transistors

Woong-Ki Hong^{1,4}, Jongwon Yoon^{2,4} and Takhee Lee³

¹ Jeonju Center, Korea Basic Science Institute, Jeonju, Jeollabuk-do 561-180, Korea

² School of Materials Science and Engineering, Gwangju Institute of Science and Technology, Gwangju 500-712, Korea

³ Department of Physics and Astronomy, and Institute of Applied Physics, Seoul National University, Seoul 151-744, Korea

E-mail: wkh27@kbsi.re.kr and tlee@snu.ac.kr

Received 22 December 2014, revised 2 February 2015

Accepted for publication 12 February 2015

Published 4 March 2015



CrossMark

Abstract

We investigated the effects of hydrogen plasma treatment on the electrical transport properties of ZnO nanowire field effect transistors (FETs) with a back gate configuration. After hydrogen plasma treatment of the FET devices, the effective carrier density and mobility of the nanowire FETs increased with a threshold voltage shift toward a negative gate bias direction. This can be attributed to the desorption of oxygen molecules adsorbed on the surface of the nanowire channel, to passivation and to doping effects due to the incorporation of energetic hydrogen ions generated in plasma.

Keywords: ZnO nanowire, electrical transport, hydrogen plasma

(Some figures may appear in colour only in the online journal)

1. Introduction

In recent years, ZnO nanostructures have attracted great attention as one of the building blocks for nanoelectronics and optoelectronics due to their unique properties such as piezoelectricity, a wide direct band gap (~ 3.37 eV) and large exciton binding energy (60 meV) [1–5]. The well-developed growth techniques of ZnO nanostructures, including the chemical vapor deposition or hydrothermal method, have allowed them to demonstrate their potential in photodetectors [6], field-effect transistors (FETs) [7], logic circuits [8], solar cells [9], nanogenerators [10] and other applications. Among those applications, FETs, as fundamental elements in nanoelectronic device applications, are particularly important.

In spite of recent great progress in synthesis methods and device applications, controlling and modifying the optical and electrical properties of ZnO nanowires still remain a challenge for the realization of high-performance device applications based on ZnO nanostructures because their properties

strongly depend on the size and shape effects of nanowires, the surface structures or surface states and the adsorption/desorption of oxygen or the water species [11–13]. To date, much research effort has been made to improve the performance of devices via surface fictionalization [14], doping [15], irradiation-induced modification [16, 17], surface passivation [12, 13], annealing [18] and especially plasma treatment [1–3, 5, 19]. Plasma treatment is one of the most effective methods for the surface modification of ZnO materials in both types of thin films and nanowires [1–5, 20, 21]. Recently, hydrogen plasma treatment has been introduced to tailor and improve the electrical and optical properties of ZnO materials and their based device properties [1–5, 20, 21]. However, to our knowledge, there have not been any reports on the influence of the hydrogen plasma treatment on the electrical transport properties of FET devices based on ZnO nanowires.

In this study, we report on the effects of hydrogen plasma treatment on the electrical transport properties of ZnO nanowire FETs. After hydrogen plasma treatment, the effective carrier density and mobility of ZnO nanowire FETs increased

⁴ These authors contributed equally to this work.

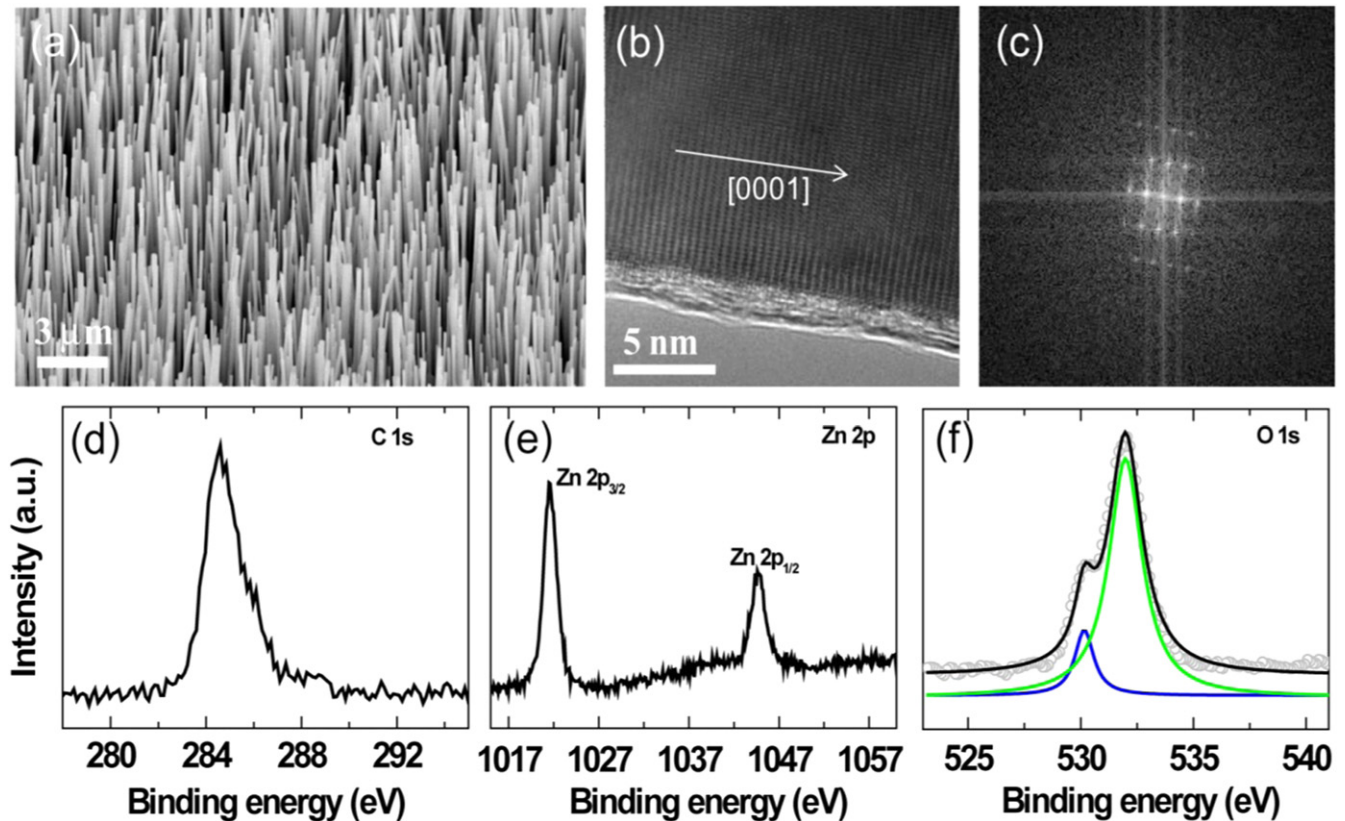


Figure 1. (a) A SEM image of as-grown ZnO nanowires on a Au-coated sapphire substrate. (b) A high-resolution TEM image of an individual ZnO nanowire and (c) its corresponding SAED pattern. XPS spectra of as-grown ZnO nanowires corresponding to (d) C 1s, (e) Zn 2p and (f) O 1s.

with a threshold voltage shift toward a negative gate bias direction. This can be explained by the desorption of oxygen molecules on the channel surface of the ZnO nanowire FETs, by passivation and by doping effects due to the incorporation of energetic hydrogen ions generated in plasma. Our study may provide useful information for tailoring the electrical characteristics of the devices based on semiconducting nanomaterials for versatile applications.

2. Experimental details

ZnO nanowires were synthesized in the horizontal tube furnace using a vapor transport method [7, 16]. Firstly, a *c*-plane sapphire substrate with a 3 nm thick gold film as a catalyst and a mixed source with a 1:1 weight ratio of commercial ZnO powder (99.995%) and graphite powder (99%) were placed on an alumina boat and positioned at the center of a tube furnace at a temperature of 930 °C for 30 min under a flow of Ar (50 sccm) and O₂ (0.2 sccm). After finishing the reaction, the ZnO nanowires were vertically and densely ordered on the Au-coated sapphire substrate (figure 1(a)). Note that as shown in figure 1(a), the Au catalysts were not observed in all the as-grown ZnO nanowires used in this study, suggesting that there is no possibility of Au contamination. The morphological and structural characterizations were performed using field emission scanning electron

microscopy (FESEM) and transmission electron microscopy (TEM). The chemical structure and composition of as-grown ZnO nanowires were examined using x-ray photoelectron spectroscopy (XPS). In order to investigate the influence of hydrogen plasma treatment (referred to as H-plasma treatment) of the electrical transport properties of ZnO nanowires, we fabricated the FET devices with a back gate configuration. The ZnO nanowires that were grown on the Au-coated sapphire substrate were transferred to a silicon wafer with 100 nm thick thermally grown silicon dioxide (SiO₂) by dropping and drying a liquid suspension of ZnO nanowires. The nanowire suspension was made by sonicating the growth substrate of ZnO nanowires in isopropyl alcohol for approximately 60 s. The highly doped p-type silicon wafers used in this study were used as a back gate electrode. For all the fabricated ZnO nanowire FETs, metal electrodes consisting of Ti (100 nm)/Au (100 nm) were deposited by an electron beam evaporator and defined as source and drain electrodes by photolithography and a lift-off process. The distance between the source and drain electrodes was approximately 3 μm (figures 2(a) and (b)). After that, we systematically measured the electrical transport properties of ZnO nanowire FETs before and after H-plasma treatment. The H-plasma treatment was performed for 120 s under a flow rate of hydrogen gas of 30 sccm and a pressure of 20 mTorr using an inductively coupled plasma system with a power of 1000 W. For the electrical measurements of the ZnO

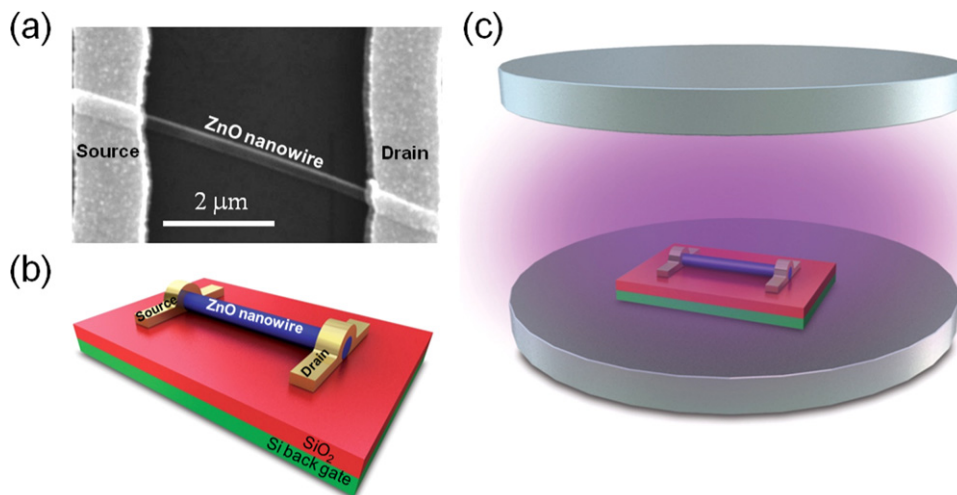


Figure 2. (a) A SEM top-view image and (b) a schematic drawing of a ZnO nanowire FET device. (c) Schematic illustration of the fabricated ZnO nanowire irradiated by hydrogen plasma.

nanowire FETs, ten devices were fabricated and characterized. The electrical properties of the nanowire FET devices were characterized using a semiconductor characterization system (Keithley 4200-SCS) at room temperature under ambient air. It should be noted that aging effects were not explored here, but future works would require a more detailed investigation of aging effects on the device's performances in ambient air.

3. Results and discussion

Figure 1(a) shows a SEM image of vertically aligned ZnO nanowires grown on the Au-coated sapphire substrate. Figures 1(b) and (c) show a high-resolution TEM image of an individual ZnO nanowire and its corresponding fast Fourier transform (FFT) electron diffraction pattern, respectively, indicating that the as-grown ZnO nanowires have a single crystalline structure with a preferential growth direction of [0001]. As shown in figures 1(d)–(f), the compositions of the as-grown ZnO nanowires were analyzed by XPS spectra in which the characteristic peaks at 1021 eV, 1044 eV and 530.1 eV correspond to the Zn $2p_{3/2}$, Zn $2p_{1/2}$ and O 1s, respectively. Note that binding energy values were specified with reference to the C 1s peak of carbon at 284.6 eV (figure 1(d)). In figure 1(f), the deconvolution of the O 1s core level XPS spectra for the as-grown ZnO nanowires shows the presence of two different peaks at 530.1 and 531.9 eV. The main peak at 530.0 eV can be attributed to the O 1s core level in the ZnO; the second peak at 531.9 eV can be associated with the presence of partially reduced ZnO (ZnO_x) or Zn-OH [22–24].

In order to investigate the hydrogen plasma effect on the electrical transport properties of the ZnO nanowires, we characterized FET devices made from as-grown ZnO nanowires before and after H-plasma treatment. Figures 2(a) and (b) show a top-view SEM image and a schematic illustration of the ZnO nanowire FET device with a back gate

configuration, respectively. As shown in figure 2(c), the H-plasma treatment was performed for 120 s under a flow rate of hydrogen gas of 30 sccm and a pressure of 20 mtorr. Additionally, we examined capacitance-gate voltage characteristics before and after H-plasma treatment after fabricating a metal-oxide-semiconductor (aluminum-SiO₂-Si back gate) structure to confirm a possibility of modification in a SiO₂ layer after H-plasma treatment. Note that the capacitance change after H-plasma treatment is negligibly small (data not shown).

Figure 3 shows representative output characteristics (source-drain current versus source-drain voltage, $I_{DS}-V_{DS}$) and transfer characteristics (source-drain current versus gate voltage, $I_{DS}-V_G$) before and after the H-plasma treatment. Figures 3(a) and (c) show typical $I_{DS}-V_{DS}$ curves obtained at V_G values ranging from -10 to $+10$ V with a step of 4 V before and after H-plasma treatment, respectively. The $I_{DS}-V_{DS}$ curves of the ZnO nanowire FET before H-plasma treatment have well-defined linear regimes at low biases and saturation regimes at high biases, indicating the Ohmic contact characteristics of the ZnO nanowire and Ti/Au electrodes [7]. Figures 3(b) and (d) also show typical $I_{DS}-V_G$ curves obtained at V_{DS} values ranging from 0.01 to 0.1 V with a step of 0.01 V before and after H-plasma treatment, respectively. The drain current (I_{DS}) increases with the increasing V_{DS} and becomes larger when a larger positive V_G is applied, which indicates an n-type semiconducting behavior [7]. From the $I-V$ characteristics (figure 3), it is clearly evident that the FET device after H-plasma treatment exhibits higher ON currents and more negative threshold voltages. Specifically, for the FET device after H-plasma treatment (figure 3(c)), the I_{DS} was significantly increased with the increasing V_{DS} compared with the FET device before H-plasma treatment (figure 3(a)). Furthermore, in $I_{DS}-V_G$ curves, the threshold voltage was shifted to a negative gate voltage direction, and the drain current value was noticeably increased after the H-plasma treatment (for example, from 37 to 81 nA at $V_G=0$ V). These results can be attributed to a larger cross-sectional area (effective channel width) in ZnO nanowires after H-plasma

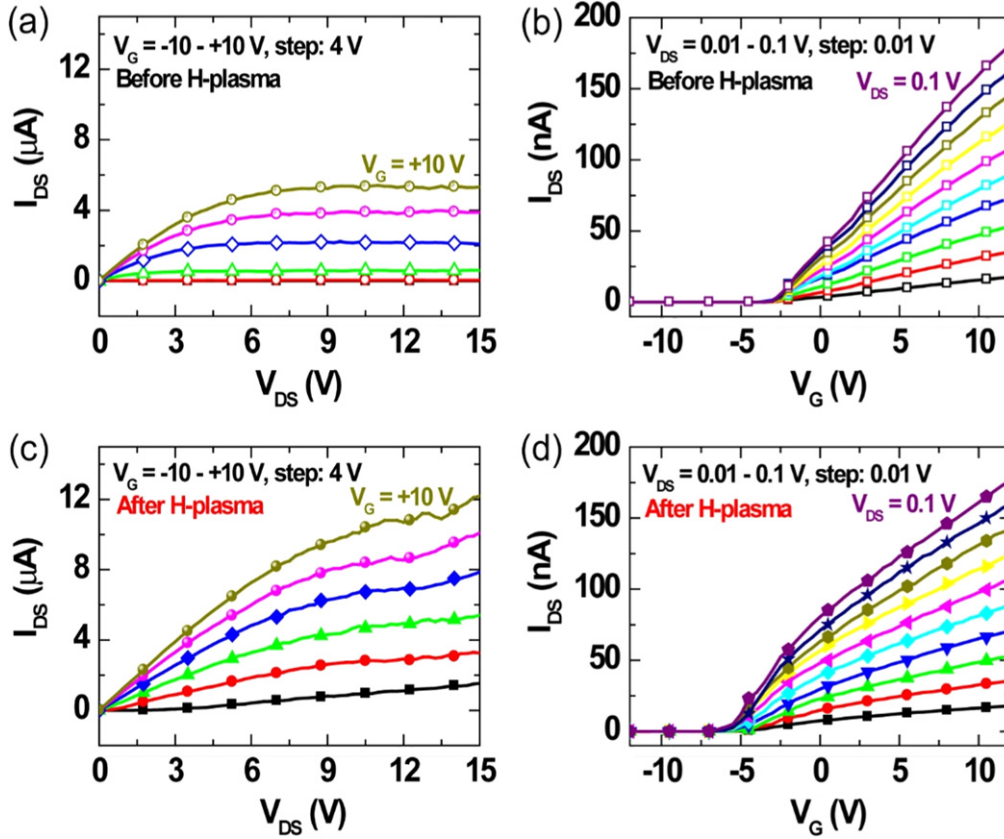


Figure 3. (a), (c) Output characteristics (I_{DS} – V_{DS}) and (b), (d) transfer characteristics (I_{DS} – V_G) of a ZnO nanowire FET before and after H-plasma treatment.

treatment, which could be indicative of the decreased surface depletion and the increased density of electron carriers in the ZnO nanowire channel by H-plasma treatment. In addition, the distinct properties of the FET device after H-plasma treatment may be attributed to the enhanced electrons–phonon (crystal lattice) scattering and/or the enhanced impurity scattering due to hydrogen doping for ZnO nanowires with a high surface area to volume ratio.

To further verify the hydrogen plasma-mediated modification of the electrical transport properties of the ZnO nanowires, we statistically examined 10 FETs and compared the changes in the electrical characteristics, as shown in figure 4. Figure 4(a) shows the representative transfer characteristics at $V_{DS}=0.1$ V in which the threshold voltage shifts toward a negative gate bias direction after H-plasma treatment. Figure 4(b) shows the statistical results of the changes in the threshold voltage and the carrier density in the nanowire channel before and after H-plasma treatment of a total of 10 ZnO nanowire FET devices characterized. The threshold voltage is defined as the gate voltage obtained by extrapolating the linear portion of the transfer characteristics (I_{DS} – V_G) from the point of maximum slope to zero drain current in which the point of maximum slope is the point where g_m is a maximum value [25]. The carrier density was estimated from the below equations [7, 25]

$$n_e = C_G(V_G - V_{th}) \quad (1)$$

$$C_G = \frac{2\pi\epsilon_r\epsilon_0L}{\cosh^{-1}\left(\frac{r+h}{r}\right)}, \quad (2)$$

where n_e is the carrier density, C_G is the gate capacitance, ϵ_r and ϵ_0 are the dielectric constant of the gate insulator (SiO_2 , 3.9) and the permittivity of the vacuum, L is the channel length ($3\ \mu\text{m}$), r is the diameter of the ZnO nanowire (50 nm) and h is the thickness of the gate insulator (100 nm). After H-plasma treatment of the ZnO nanowire FETs, the threshold voltage shifted toward a negative gate voltage direction from -2.8 to -5.8 V, as shown in figure 4(a). Then, the carrier density before and after H-plasma treatment was 1.3×10^{18} and $1.6 \times 10^{18}\ \text{cm}^{-3}$ at $V_G=10$ V, respectively. In figure 4(b), the average threshold voltage and the average carrier density were determined to be approximately 2.3 V and $7.5 \times 10^{17}\ \text{cm}^{-3}$, -6.6 V and $1.6 \times 10^{18}\ \text{cm}^{-3}$ before and after H-plasma treatment, respectively. This indicates that shallow donors can be formed by H-plasma treatment [1, 2, 4]. Figures 4(c) and (d) show contour plots of field-effect mobility (μ_{FE}) and transconductance (g_m), respectively, as a function of drain and gate bias voltages before and after H-plasma treatment. The μ_{FE} can be calculated by using equations (2) and (3) [7, 25]

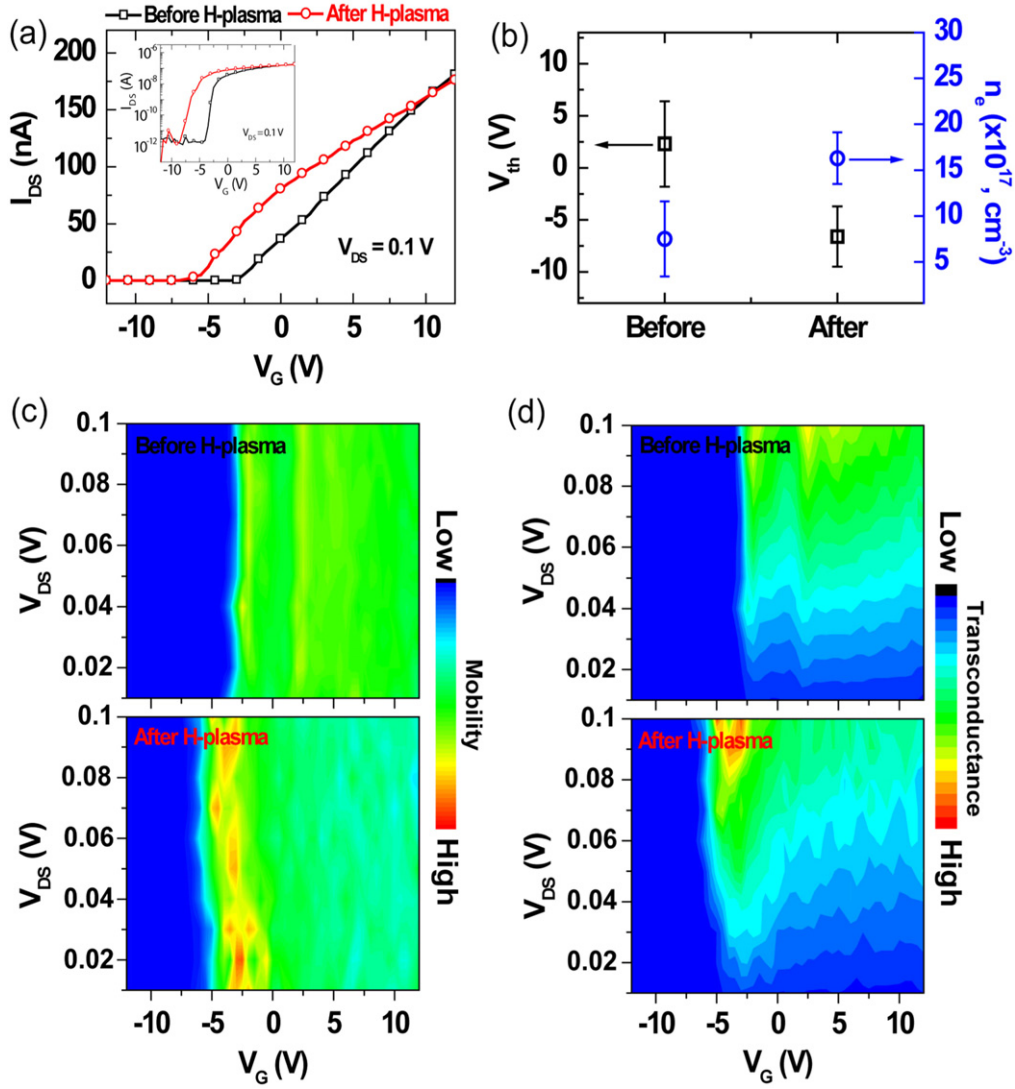


Figure 4. (a) Representative transfer characteristics (I_{DS} - V_G) at $V_{DS}=0.1$ V for a ZnO nanowire FET before and after H-plasma treatment. The inset shows the semi-logarithmic plot of the I_{DS} - V_G curves at $V_{DS}=0.1$ V before and after H-plasma treatment. (b) The threshold voltage (V_{th}) shift and the change in carrier concentration (n_e) for the ZnO nanowire FETs before and after H-plasma treatment. The contour plots of (c) transconductance (g_m) and (d) field-effect mobility (μ_{FE}) as a function of V_{DS} and V_G for a ZnO nanowire FET before and after H-plasma treatment.

$$\mu_{FE} = \frac{dI_{DS}}{dV_G} \frac{L^2}{V_{DS}C_G}, \quad (3)$$

where the transconductance ($g_m = dI_{DS}/dV_G$) was obtained from transfer characteristics (I_{DS} - V_G) (figures 3(b) and (d)). It should be noted that since the μ_{FE} is deduced from the g_m and V_{th} in the I - V characteristics, a difficulty in the accurate assessment of the μ_{FE} can arise from the error associated with finding V_{th} and g_m from the measured I - V characteristics. In figures 4(c) and (d), the maximum values of carrier mobility and transconductance at the critical gate bias voltages (or electric field) after H-plasma treatment are relatively much larger than those before H-plasma treatment. This implies that H-plasma treatment can lead to the passivation of defects, resulting in the suppression of the oxygen absorption on the nanowire's surface. Notably, compared with the FET device before H-plasma treatment,

changes in mobility and transconductance of the FET device after H-plasma treatment strongly depend on an increase with the electric field, which causes carriers to be drawn closer to the interface between the ZnO nanowire and a SiO_2 layer. The mobility and transconductance changes as a function of voltage for all measured nanowire FETs exhibit a similar behavior with at first increasing with V_G before decaying at high gate voltages. The interesting thing here is that for the H-plasma-treated FET devices, the mobility and transconductance more sharply decay at high gate voltages. This distinct decay can be attributed to the enhanced scattering of the electrons at high gate voltages, which is similar to the behavior that is observed in conventional Si MOSFETs. The device parameters of ZnO nanowire FETs before and after H-plasma treatment are summarized in table 1. In table 1, the enhancement of the mobility, transconductance, carrier concentration and on/off

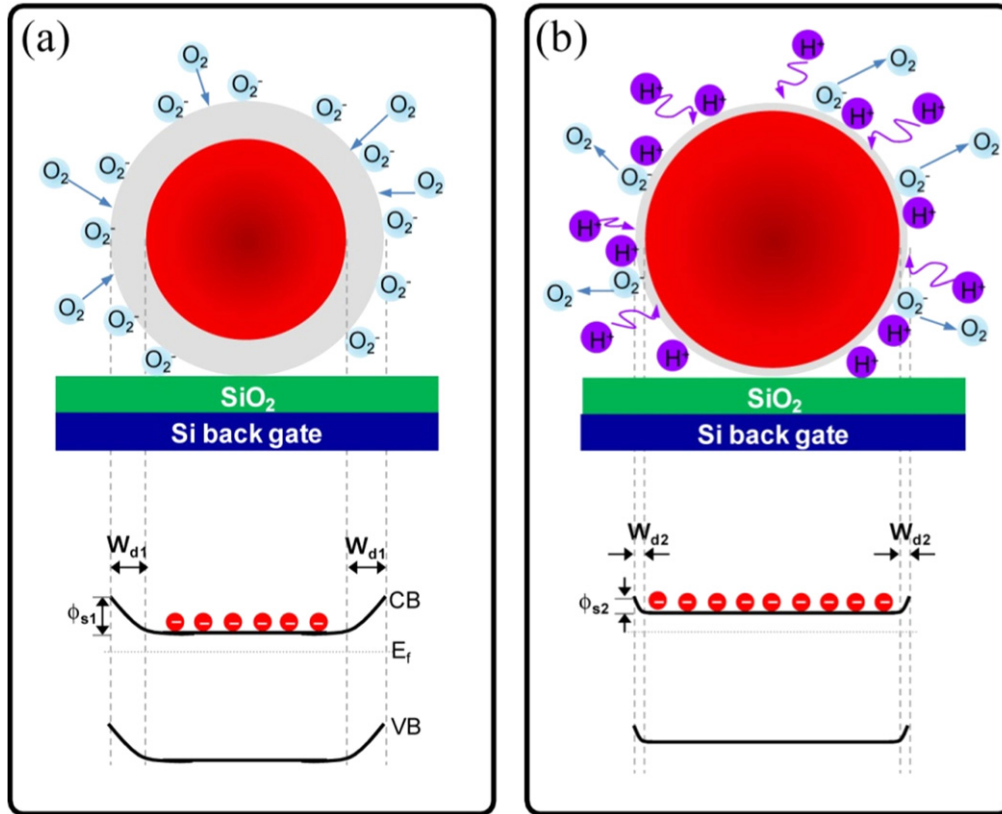


Figure 5. (Top) Cross-sectional schematic illustrations and (bottom) the corresponding energy band diagrams for ZnO nanowire FETs before and after H-plasma treatment.

Table 1. Comparison of device parameters between the ZnO nanowire FETs before and after H-plasma treatment.

	V_{th} (V)	$g_{m,max}$ (nS)	μ_{FE} ($\text{cm}^2 \text{Vs}^{-1}$)	n_e ($\times 10^{17} \text{cm}^{-3}$)	SS (V/dec)	I_{on}/I_{off} ($\times 10^6$)
Before H-plasma	2.3 ± 4.1	26.8 ± 16.2	65.5 ± 39.5	7.5 ± 4.1	0.39 ± 0.04	1.1 ± 1.5
After H-plasma	-6.6 ± 2.9	36.1 ± 23.6	88.2 ± 57.7	16.3 ± 2.8	0.88 ± 0.21	2.6 ± 1.9

current ratio for the H-plasma-treated ZnO nanowire FETs are indicative of the enhancement of device performance of FETs by H-plasma treatment. As an important device performance parameter of the FET device, the subthreshold swing (SS), defined as $SS = dV_G/d\log I_{DS}$, is desired to be small for low-power operation. The SS for H-plasma-treated FETs is relatively larger compared to the FET device before H-plasma, implying that the electron carriers in the channel after H-plasma treatment undergo increased surface scattering, including the scattering with the crystal lattice (phonon) and ionized impurity atoms.

Here, the experimental observations of the influence of H-plasma treatment on the electrical properties of the ZnO nanowire FETs studied can be explained using an energy band structure, as shown in figure 5. As reported previously, a great number of oxygen molecules can be adsorbed on a lot of adsorbed sites on the nanowire's surface due to a high surface area to volume ratio [7, 16, 25]. Accordingly, free electrons of the nanowire channel are trapped at the nanowire's surface due to the adsorption of oxygen molecules (figure 5(a), top), resulting in the energy band structure with a relatively larger

surface depletion width (W_{d1}) and higher surface potential (ϕ_{s1}) (figure 5(a), bottom). In contrast, the energy band structure observed after H-plasma treatment (figure 5(b), bottom) shows a relatively smaller surface depletion width (W_{d2}) and lower surface potential (ϕ_{s2}), resulting from the desorption of oxygen ions from the surface of the nanowire channel due to energetic ion bombardment (figure 5(b), top). Additionally, the exposure of ZnO to the hydrogen plasma leads to the passivation effect of the defects and the doping effect of shallow donors [1, 2]. Consequently, the H-plasma treatment causes the threshold voltage to shift toward the negative gate bias direction and results in the enhancement of electrical conductance under the same applied gate bias due to the increase in carrier density. Correspondingly, considering donor density (N_d) and trapped-charge density (N_t) in ZnO nanowires, we further calculated the depletion width and surface potential by using the depletion approximation and charge neutrality condition [26–28], which can be described by $W_d = (2\epsilon_{ZnO}\phi_s/qN_d)^{1/2}$ and $N_t = 2N_dW_d$, where ϕ_s is the surface potential, q is the electronic charge, N_d is the doping density and ϵ_{ZnO} is the dielectric constant of ZnO (8.66) [29].

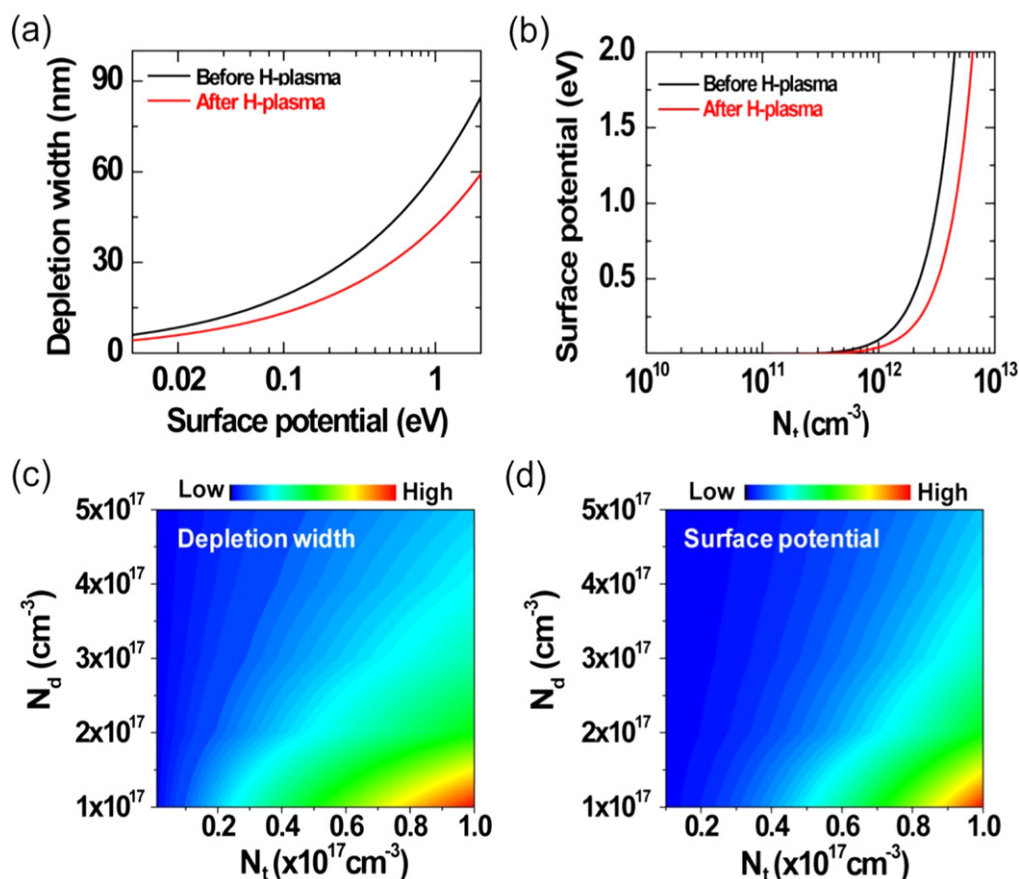


Figure 6. (a) Depletion width as a function of surface potential and (b) surface potential as a function of trapped-charge density of ZnO nanowires before and after H-plasma treatment. Contour plots of the depletion width (c) and surface potential (d) as a function of trapped-charge and doping density, respectively.

By assuming that the N_d is the carrier density at $V_G=0$ V, that the ZnO nanowires are cylindrical in shape and that the equivalent depletion region is formed due to the surface states, the calculated results of the depletion width as a function of surface potential and the surface potential as a function of trapped-charge density can be estimated, as shown in figures 6(a) and (b). Figures 6(c) and (d) also show the contour plots of depletion width and surface potential as a function of trapped-charge density for the N_d ranges from 1×10^{17} – $5 \times 10^{17} \text{cm}^{-3}$. This implies that the electrical transport properties are affected by the surface modification of the nanowire channel by H-plasma treatment, leading to the change in charge density, surface depletion and surface potential.

4. Conclusion

In summary, we investigated the modification of the electrical transport properties of the ZnO nanowire FETs before and after H-plasma treatment. After H-plasma treatment, the threshold voltage of the FET devices shifted toward the negative gate bias direction, and the carrier density and mobility were improved. The result can be explained by the modification of the energy band structure due to the desorption of oxygen molecules absorbed on the surface of the

ZnO nanowire channel, by passivation and by doping effects induced by energetic hydrogen ions generated in plasma. Our study may provide useful information for the further study of plasma-induced charge transport of other semiconducting nanomaterials and for developing high-performance electronic device applications.

Acknowledgments

W K H acknowledges the financial support from the Korea Basic Science Institute (KBSI) (Grant No. T34516) and the National Research Foundation of Korea (NRF), funded by the Ministry of Education (No. NRF-2014M2B2A4030807). T L acknowledges the financial support of the National Creative Research Laboratory Program (Grant No. 2012026372), funded by the Korean Ministry of Science, ICT & Future Planning.

References

- [1] Dong J J, Zhang X W, You J B, Cai P F, Yin Z G, An Q, Ma X B, Jin P, Wang Z G and Chu P K 2010 *ACS Appl. Mater. Interfaces* **2** 1780
- [2] Li Y, Zhong M, Tokizono T, Yamada I, Bremond G and Delaunay J-J 2011 *Nanotechnology* **22** 435703

- [3] Lai C-Y, Chien T-C, Lin T-Y, Ke T, Hsu S-H, Lee Y-J, Su C-Y, Sheu J-T and Yeh P-H 2014 *Nanoscale Res. Lett.* **9** 281
- [4] Polyakov A Y *et al* 2003 *J. Appl. Phys. Lett.* **94** 3960
- [5] Baratto C, Comini E, Ferroni M, Faglia G and Sberveglieri G 2013 *Cyst. Eng. Comm.* **15** 7981
- [6] Zhou J, Gu Y, Hu Y, Mai W, Yeh P-H, Bao G, Sood A K, Polla D L and Wang Z L 2009 *Appl. Phys. Lett.* **94** 191103
- [7] Hong W-K, Hwang D-K, Park I-K, Jo G, Song S, Park S-J, Lee T, Kim B-J and Stach E A 2007 *Appl. Phys. Lett.* **90** 243103
- [8] Jo G, Hong W-K, Maeng J, Choe M, Park W and Lee T 2009 *Appl. Phys. Lett.* **94** 173118
- [9] Law M, Greene L E, Johnson J C, Saykally R and Yang P 2005 *Nat. Mater.* **4** 455
- [10] Sohn J I *et al* 2013 *Energy Environ. Sci.* **6** 97
- [11] Soci C, Zhang A, Xiang B, Dayeh S A, Aplin D P R, Park J, Bao X Y, Lo Y H and Wang D 2007 *Nano Lett.* **7** 1003
- [12] Song S, Hong W-K, Kwon S-S and Lee T 2008 *Appl. Phys. Lett.* **92** 263109
- [13] Chen Q, Ding H, Wu Y, Sui M, Lu W, Wang B, Su W, Cui Z and Chen L 2013 *Nanoscale* **5** 4162
- [14] Lin M C, Chu C J, Tsai L C, Lin H Y, Wu C S, Wu Y P, Wu Y N, Shieh D B, Su Y W and Chen C D 2007 *Nano Lett.* **7** 3656
- [15] Sohn J I, Jung Y-I, Baek S-H, Cha S N, Jang J E, Cho C-H, Kim J H, Kim J M and Park I-K 2014 *Nanoscale* **6** 2046
- [16] Hong W-K, Jo G, Sohn J I, Park W, Choe M, Wang G, Kahng Y H, Welland M E and Lee T 2010 *ACS Nano* **4** 811
- [17] Li W *et al* 2014 *Nano Res.* **7** 1691
- [18] Keem K, Kang J, Yoon C, Jeong D-Y, Moon B-M and Kim S 2007 *Jpn. J. Appl. Phys.* **46** 6230
- [19] Kim S, Kim H, Janes D B and Ju S 2013 *Nanotechnology* **24** 305201
- [20] Lee D-M, Kim J-K, Hao J, Kim H-K, Yoon J-S and Lee J-M 2014 *J. Alloy Compd.* **583** 535
- [21] Wang F-H, Chang H-P, Tseng C-C, Huang C-C and Liu H-W 2011 *Curr. App. Phys.* **11** S12
- [22] Yang X J, Miao X Y, Xu X L, Xu C M, Xu J and Liu H T 2005 *Opt. Mater.* **27** 1602
- [23] Chen M, Wang X, Yu Y H, Pei Z L, Bai X D, Sun C, Huang R F and Wen L S 2000 *Appl. Surf. Sci.* **158** 134
- [24] Armelao L, Fabrizio M, Gialanella S and Zordan F 2001 *Thin Solid Films* **394** 90
- [25] Hong W-K, Jo G, Kwon S-S, Song S and Lee T 2008 *IEEE Trans. Electron. Dev.* **55** 3020
- [26] Goldberger J, Sirbully D J, Law M and Yang P 2005 *J. Phys. Chem. B* **109** 9
- [27] Yu P Y and Cardona M 2001 *Fundamentals of Semiconductors: Physics and Materials Properties* (Berlin: Springer-Verlag) pp 445–53
- [28] Taur Y and Ning T H 1998 *Fundamentals of Modern VLSI Devices* (Cambridge: Cambridge University Press) pp 63–7
- [29] Fan Z and Lu J G 2005 *Nanosci. Nanotechnol.* **5** 1561